

UV-crosslinked glyoxal-methacrylate electrolytes for quasi-solid electric double layer capacitors

*Original*

UV-crosslinked glyoxal-methacrylate electrolytes for quasi-solid electric double layer capacitors / Porporato, S., Luis Gomez-Urbano, J., Piovano, A., Elia, G.A., Gerbaldi, C., Balducci, A.. - In: ELECTROCHIMICA ACTA. - ISSN 0013-4686. - STAMPA. - 525:(2025). [[10.1016/j.electacta.2025.146096](https://doi.org/10.1016/j.electacta.2025.146096)]

*Availability:*

This version is available at: 11583/2998652 since: 2025-03-29T20:37:23Z

*Publisher:*

Elsevier

*Published*

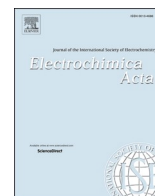
DOI:[10.1016/j.electacta.2025.146096](https://doi.org/10.1016/j.electacta.2025.146096)

*Terms of use:*

This article is made available under terms and conditions as specified in the corresponding bibliographic description in the repository

*Publisher copyright*

(Article begins on next page)



# UV-crosslinked glyoxal-methacrylate electrolytes for quasi-solid electric double layer capacitors

Silvia Porporato<sup>a,b</sup>, Juan Luis Gómez-Urbano<sup>c</sup>, Alessandro Piovano<sup>a,b</sup>, Giuseppe A. Elia<sup>a,b</sup>, Claudio Gerbaldi<sup>a,b,\*</sup> , Andrea Balducci<sup>c,\*</sup>

<sup>a</sup> GAME Lab, Department of Applied Science and Technology (DISAT), Politecnico di Torino, Corso Duca degli Abruzzi, 24, 10129 Torino, Italy

<sup>b</sup> National Reference Centre for Electrochemical Energy Storage (GISEL) - INSTM, Via G. Giusti 9, 50121 Firenze, Italy

<sup>c</sup> Institute for Technical Chemistry and Environmental Chemistry (ITUC) and Center for Energy and Environmental Chemistry Jena (CEEC), Philosophenweg 7a, 07743 Jena, Germany

## ARTICLE INFO

### Keywords:

Electric double layer capacitor  
Sodium  
Gel polymer electrolyte  
Glyoxal  
Methacrylate  
UV crosslinking

## ABSTRACT

In this paper, the difunctional oligomer bisphenol A ethoxylate dimethacrylate (BEMA), known for readily undergo UV-induced polymerisation, is employed to produce a highly crosslinked polymer network, in combination with poly(ethylene glycol) methyl ether methacrylate (PEGMEMA) as a reactive diluent. The methacrylate-based membranes are soaked with a low-volatile glyoxal-based electrolyte, namely 1 M sodium bis(trifluoromethanesulfonyl)imide (NaTFSI) in a 3:7 mixture of tetraethoxyglyoxal (TEG) and propylene carbonate (PC), respectively. The resulting gel polymer electrolytes are successfully employed for the fabrication of laboratory-scale quasi-solid electric double layer capacitors (EDLCs), showing sufficient thermal stability, high ionic conductivity at different temperatures, suitable electrochemical stability window and stable prolonged constant-current cycling (high capacitance up to  $21 \text{ F g}^{-1}$  at  $0.2 \text{ A g}^{-1}$  with excellent efficiency for thousands of cycles and  $>85\%$  of capacitance retention after a rate capability test and 9500 reversible cycles), thus paving the way for further detailed studies and optimizations.

## 1. Introduction

The development of electrochemical energy storage devices providing high energy and power densities is required to fulfill the increasing global demand for electricity production/use in multiple applications, including electric vehicles or grid storage for renewable energy sources [1,2]. The charge in these devices can be stored through two distinct processes, generally either via a non-faradaic process or via a faradaic one. In the latter case, charges are stored through the faradaic oxidation and reduction of electrochemically active species, namely the active materials in the electrodes (e.g. pseudocapacitors, batteries) [3]. Instead, non-faradic devices rely on the polarization of charges at the surface of the electrodes, representing a rapid and confined physical phenomenon; charges are electrostatically stored, and no chemical reactions occur. Electrochemical double layer capacitors (EDLC), also known as supercapacitors, are the main representative of this type of technology [4–7].

Since EDLCs rely on a physical storage mechanism, the formation of the electrochemical double-layer at the interface between electrodes and

electrolyte takes place in a very short period, generally in the range of seconds or below, facilitating an elevated specific power density ( $>10 \text{ kW kg}^{-1}$ ). Moreover, the absence of redox reactions minimizes degradation phenomena, enabling a significantly higher cycle life ( $>500,000$  cycles) if compared to faradic devices. On the other hand, the charge storage process in EDLCs is a surface-limited phenomenon, considerably limiting their energy density to values in the range of  $5 \text{ Wh kg}^{-1}$  [8–10]. In this regard, the development of high-energy EDLCs has attracted considerable attention to fully exploit the previously mentioned characteristics that make them the devices of choice for a large variety of high-power applications.

Despite great efforts have been made to enhance the energy output of these devices through the development of high-surface area electrodes (i.e., activated carbons), the role of the electrolyte should be carefully considered. Generally, liquid organic electrolytes are the preferred option for commercial EDLCs. In this regard, 1 M tetraethylammonium tetrafluoroborate ( $\text{Et}_4\text{NBF}_4$ ) in acetonitrile (ACN) is amongst the most widely used formulations due to its high ionic conductivity and wide electrochemical stability window (ESW) [11]. ACN offers also low

\* Corresponding authors.

E-mail addresses: [claudio.gerbaldi@polito.it](mailto:claudio.gerbaldi@polito.it) (C. Gerbaldi), [andrea.balducci@uni-jena.de](mailto:andrea.balducci@uni-jena.de) (A. Balducci).

viscosity, which enhances ion mobility, but is a flammable and toxic solvent, which raises safety and environmental concerns upon leakage [12]. On the other hand, an ideal electrolyte should present low toxicity, reduced flammability, chemical and electrochemical stability, environmental degradability, ease of manufacturing, abundance of its raw materials and low cost [11].

To avoid these issues while concurrently enhancing specific characteristics, solid polymer electrolytes (SPEs) have steadily gained ground in the last decades. SPEs mainly consist of an alkali metal salt dissolved in a polymer matrix, which not only avoids electrolyte leakage but also can substitute the cell separator, thus saving costs from the overall cell manufacturing process [13]. So far, poly(ethylene oxide) (PEO)-based systems are the most studied and common technology [14]. PEO shows a high solubility for salts without phase separation and, in general, PEO-based systems allow for the fabrication of light-weight, self-standing and flexible solid-state systems. Unfortunately, PEO crystallizes below  $\sim 60$  °C and possesses limited  $\text{Li}^+/\text{Na}^+$  transport number and oxidative stability [15]. To overcome limitations associated to PEO, a large number of different polymers have been investigated as host systems for SPEs, such as poly(methyl methacrylate), poly(acrylonitrile), poly(-vinylidene fluoride) or other various co-polymers [16]. Among them, methacrylate-based systems have the advantage of wide availability, low toxicity and good electrochemical stability towards both reduction and oxidation reactions [17].

Nevertheless, in spite of several decades of study, the overall conductivity of SPEs remains below the required threshold values for most energy storage applications [18,19]. Thus, to combine the high ionic conductivity of liquid electrolytes with the advantages of SPEs mentioned above, gel polymer electrolytes (GPEs) have been introduced. In these systems, a liquid electrolyte is immobilized into a polymer matrix. In this way, adequate conductivity can be achieved, while also preserving mechanical integrity, thus enabling their use as safer separating electrolyte in electrochemical energy storage devices [20].

GPEs can be prepared in many ways, depending on the precursor materials and envisaged applications. In the simplest case, a liquid electrolyte solution is trapped within a thermoplastic polymer to improve significantly ionic conductivity. Such a preparation is time/energy-consuming, and, once formed, the membranes may dissolve in the same solvent, especially at high temperatures. An appealing alternative is based on UV-induced crosslinking, which is a photoinduced polymerization technique operated at room temperature. In this well-established process, a liquid monomer is mixed with an appropriate photoinitiator, evolving into a highly crosslinked solid film when irradiated with UV-light for a short period of time (seconds to minutes). A typical formulation may contain multiple monomers, but is usually solvents-/catalysts-free. As a result, this process is both rapid and environmentally friendly, with low energy consumption and no emission of volatile organic compounds [17,21,22].

In particular, methacrylate-based GPEs can be manufactured by direct UV-light irradiation of a liquid precursor mixture of the electrolyte components “in one pot” [17,23,24]. Amongst the variety of methacrylate compounds available, bisphenol A ethoxylate dimethacrylate (BEMA) is a methacrylic-based difunctional oligomer that readily polymerizes by UV-curing, resulting in the formation of highly crosslinked polymer networks, flexible and resistant up to 300 °C [24, 25]. Poly(ethylene glycol) methylether methacrylate (PEGMEMA) is a monofunctional monomer, normally used in polymer science as a reactive diluent [24], to control the crosslinking density, and to reduce the glass transition temperature ( $T_g$ ) of the resulting membranes, thanks to the presence of pendant ethoxy groups [26]. Noteworthy, a low  $T_g$  enables the proper mobility and elasticity of the polymer chains at room temperature, consequently leading to an enhanced ionic conductivity [27].

A plethora of solvents is available to produce GPEs, most of them being toxic and flammable organic compounds, likely to be avoided in

next-generation technologies. Starting from this premise, glyoxal-acetal-derived electrolytes were firstly proposed in 2018 after a computational screening for the identification of new electrolyte components for EDLC and batteries [6,28,29]. Tetraethoxyglyoxal (TEG) is the full acetal of glyoxal (IUPAC name: oxoaldehyde) and can be obtained from the latter via a condensation reaction with methanol or ethanol [30]. Compared to commonly used carbonate-based solvents, it shows several advantages. First, the aldehydic precursor is commercially available, with a comparable price to carbonate solvents. Additionally, it is classified as harmless from an environmental point of view. Albeit the relatively not so high dielectric constant, it shows excellent thermal stability, high boiling and flash points, low viscosity, low melting point and it also has the capability to dissolve a wide range of salts. So far, TEG has been investigated in lithium-, sodium-, and potassium-ion batteries, giving promising results [30–35]. Moreover, TEG has demonstrated to form of a robust SEI layer on different carbon materials, such as graphite, soft carbon and hard carbon electrodes [33,36,37]. In addition, in a recent work, 1 M LiTFSI in TEG:PC (3:7) has been successfully used for the formulation of a novel gel-polymer-based electrolyte for Li-ion batteries [38].

In this work, we focus on the development of novel GPEs starting from a BEMA and PEGMEMA-based mixture in combination with a glyoxal-based electrolyte, namely 1 M sodium trifluoromethanesulfonimide (NaTFSI) in a 3:7 proportion between TEG and propylene carbonate (PC). This electrolyte formulation was selected because it has been shown that can be successfully utilized in Na-based systems and, therefore, represents a good reference for this study [29, 39–41]. The prepared GPEs were thoroughly characterized in terms of their thermal, morphological, electrical and electrochemical characteristics, comparing the results with liquid electrolyte, thus pointing out the different behavior of the ions within the same medium but in the presence or not of a polymeric network that affects the solvation structure [42–44]. The electrochemical investigation, including cyclic voltammetry (CV), galvanostatic cycling (GC), anodic dissolution and floating tests, demonstrated efficient long-term cycling, in laboratory-scale quasi-solid sodium-based EDLCs.

## 2. Experimental section

### 2.1. Materials

The methacrylic-based di-functional oligomer bisphenol A ethoxylate (15 EO/phenol) dimethacrylate (BEMA, average  $M_n$  1700), poly(ethylene glycol)methylether methacrylate (PEGMEMA,  $M_n$  475) and the free radical photoinitiator 2-hydroxy-2-methyl-1-phenyl-1-propanone (Darocur 1173/D1173) were purchased by Sigma Aldrich. Tetraethoxyglyoxal (TEG, Weylchem) was passed before use through a freshly activated alumina column in order to remove the stabilizer and then dried with freshly activated molecular sieves. As-dried TEG and PC (Sigma Aldrich) were utilized to prepare a binary solvent mixture with a weight ratio of 3:7. The sodium bis(trifluoromethanesulfonyl)imide (NaTFSI) salt was purchased from Solvionic. All chemicals were stored in an Ar-filled dry glove box (MBraun UniLab,  $\text{O}_2$  and  $\text{H}_2\text{O}$  content < 1 ppm) before use.

### 2.2. Gel-polymer electrolyte (GPE) membrane preparation

The preparation of the gel polymer electrolyte (GPE) membranes was based on BEMA and PEGMEMA, which were mixed in a 7:3 proportion in a dark glass vial for 30 min, as previously described by Nair et al. [26]. Successively, D1173 was added and the solution was stirred for additional 30 min. The polymeric slurry was later coated onto a silicon mold (100  $\mu\text{m}$  thick), covered with a transparent Mylar foil and irradiated with UV-light (wavelength of 395 nm) for 3 min. The resulting fully solid and transparent polymer membrane was then immersed for 2 h in 1 M NaTFSI in TEG/PC (3:7 in weight), which resulted in the final GPE,

namely GM-GPE, ready to use after gently surface drying with towel paper.

### 2.3. Thermal, electrical and morphological characterization

The thermal stability of the materials under study was measured by thermogravimetric analysis (TGA, Netzsch TG 209 F3). The analysis was conducted between 25 and 800 °C under nitrogen atmosphere (N<sub>2</sub> flux of 100 mL min<sup>-1</sup>), using a heating ramp of 10 °C min<sup>-1</sup>.

For ionic conductivity measurements, GM-GPE was placed between two stainless-steel current collectors housed in an ECC-Std (EL-Cell GmbH, Hamburg, Germany) testing cell and multiple electrochemical impedance spectroscopy (EIS) measurements were led. For the measurements, an alternating voltage signal of 20 mV within the frequency range of 200 kHz to 100 mHz was employed. The ionic conductivity ( $\sigma$ ) values were calculated from Equation 1:

$$\sigma = \frac{l}{A \cdot R} \text{ [S/m]} \quad (1)$$

where  $l$  and  $A$  represent the thickness and the effective area of the membrane respectively, and  $R$  denotes the resistance determined from the resulting Nyquist plots.

Field emission scanning electron microscopy (FESEM) images were collected with 5 keV electrons using an in-lens detector of a Zeiss SUPRA 40 (Zeiss SMT, Oberkochen, Germany).

### 2.4. Electrodes and cell preparation, electrochemical characterization

Activated carbon (AC) electrodes were produced by mixing the active material (YP50, Kuraray) with Super P C65 (C—ENERGY, Imerys) and sodium carboxymethylcellulose (NaCMC, CRT 2000 GA, Walocel) in water according to a mass ratio of 90:5:5. The water-based AC slurry was coated on aluminum foil and dried at 60 °C under vacuum overnight. Aluminum foil was etched in a 5 % (w/v) KOH solution bath at 60 °C for 1 min before casting. Electrodes with a diameter of 12 mm were punched out from the foil and dried overnight under vacuum at 65 °C before transferring them into the glove box for cell assembly. Mass loading of the AC electrodes was controlled by adjusting the wet thickness of the coater, obtaining ca. 1.30 mg cm<sup>-2</sup> per electrode. Cell assembly was carried out using Swagelok-type cells and ECC-Std test cells inside an argon-filled glovebox. The GPE served simultaneously as the separator and the electrolyte. For the assembly of the cells containing the reference liquid electrolyte (150  $\mu$ L of 1 M NaTFSI in TEG/PC), glass-fiber (Whatman GF/D) was used as separator.

The electrochemical stability window (ESW) of the GPE and liquid electrolyte was evaluated via linear sweep voltammetry (LSV) at 1 mV s<sup>-1</sup> ( $\pm 0.1$  mA cm<sup>-2</sup> current threshold) in a Swagelok-type three-electrode configuration. A platinum disc was used as working electrode, an oversized AC disc as counter electrode and a silver wire as quasi-reference electrode. The anodic dissolution tests were carried out with the same setup except for the use of a pristine aluminum disc as working electrode. During these measurements, the potential of the aluminium discs was increased 1.3 V over the open circuit potential and subsequently reverted at a scan rate of 5 mV s<sup>-1</sup>. The potential was held for 3 h at the upper potential limit of each cycle.

The AC-based electrodes were electrochemically characterized in an EDLC full-cell symmetrical configuration (two electrode set up in ECC-Std test cell) in a voltage range of 0 – 2.6 V. Cyclic voltammetry (CV) and galvanostatic charge-discharge measurements were performed on a multichannel VMP3 potentiostat/galvanostat/frequency response analyser from Biologic. Applied current density ( $I_g$ ) values were calculated on the basis of the total mass of active material ( $m_{act}$ ) in the electrodes (90wt. %). Specific capacitance ( $C_g$ ) values of the two electrode symmetric cells were calculated from the discharge galvanostatic plots, following Equation 2:

$$C_g = \frac{I_g t_d}{V} \quad (2)$$

where  $t_d$  and  $V$  are respectively the discharge time and the operational voltage window, once the total resistance drop is subtracted. Gravimetric energy ( $E_g$ ) and power densities ( $P_g$ ) were calculated accordingly to Eqs. 3 and 4:

$$E_g = \frac{1}{2} C_g \times V^2 \quad (3)$$

$$P_g = \frac{E_g}{t_d} \quad (4)$$

[45]. Floating tests were also carried out on the symmetric EDLCs by holding the cell voltage at 2.6 V. After floating for 5 h, the cells were galvanostatically cycled at 0.2 A g<sup>-1</sup> for 10 cycles from 0 to 2.6 V before holding again the voltage of the cell at the upper voltage limit. This process was repeated up to 100 h of floating.

## 3. Results and discussion

### 3.1. 3.1. Electrolyte characterization

A novel GPE consisting of methacrylate polymers and glyoxal-based electrolyte for quasi solid-state Na-based EDLCs is here developed and investigated. The thermal stability of the liquid glyoxal-based electrolyte and the GM-GPE after 2 h swelling step in the electrolyte solution was assessed by TGA under flowing nitrogen (Fig. 1a). The degradation profile of 1 M NaTFSI in TEG:PC liquid electrolyte vs. temperature agrees well with the reported literature [30], retaining 95 % of its initial mass up to 80 °C. As expected, the GM-GPE shows a first weight loss related to the removal of glyoxal-based electrolyte at ~100 °C, while the polymer structure degradation starts at 320 °C, which is in agreement with previous studies on analogous methacrylate-based polymer membranes [17,46]. Thus, degradation of the liquid electrolyte component within the GPE is retarded when comparing to that of the liquid electrolyte, which indicates that the electrolyte is efficiently encompassed in the crosslinked polymeric matrix, therefore enhancing the safety of the system. The further weight loss at approximately 450 °C can be related to the NaTFSI salt decomposition, which also appears to be delayed when the salt is encompassed within the polymer host [47]. TGA results account for the safe use of GM-GPE in practical EDLCs up to 100 °C.

Ionic conductivity tests were performed in a wide range of temperatures for 1 M NaTFSI in TEG:PC (3:7) and GM-GPE; corresponding Arrhenius plots are shown in Fig. 1b. GM-GPE shows a Vogel–Tammann–Fulcher (VTF) behavior, which is typical of fully amorphous polymer electrolytes, and is described by Equation 5:

$$\sigma = AT^{-1/2} \exp \frac{-E_a}{R(T - T_0)} \quad (5)$$

where  $\sigma$  is the ionic conductivity,  $A$  is the pre-exponential factor,  $E_a$  is the apparent activation energy of the ion transport associated with the segmental motion of the polymer,  $R$  is the Boltzmann constant, and  $T_0$  is the ideal glass transition temperature. VTF behavior is a clear indication of the strong dependence of the ion conduction on the polymer segmental motion [48,49]. The ionic conductivity of the pure 1 M NaTFSI in TEG:PC (3:7) was already investigated in a previous work [30], showing a value of 3.1 mS cm<sup>-1</sup> at 20 °C. As expected, at the same temperature, the conductivity of GM-GPE is around one order of magnitude lower (0.33 mS cm<sup>-1</sup>), but nonetheless in line or even higher compared to most of the GPEs reported in the literature [15,50].

Fig. 1c shows the Nyquist plot of the GM-GPE acquired at different temperatures, viz. -20, 20, 40 and 80 °C. Theoretically, the spectrum of an ideal capacitor is composed of a perfectly vertical line (90°), which exclusively reflects capacitive-like phenomena. In the case of the GM-

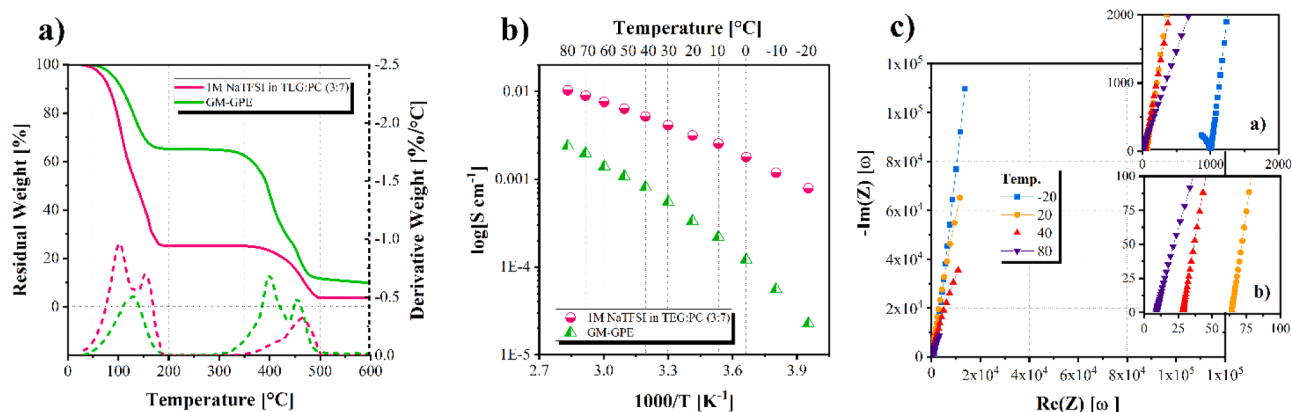


**Fig. 1.** a) TGA analysis under  $N_2$  flux (temperature range 25–800 °C) of the GM-GPE after 2 h swelling process, along with the pure liquid electrolyte. b) Arrhenius plot of the ionic conductivity vs. inverse temperature of 1 M NaTFSI in TEG:PC (3:7) and GM-GPE in the range of –20 to 70 °C, acquired every 10 °C. c) Nyquist plot of the GM-GPE at –20, 20, 40 and 80 °C. Insets a) and b) show a zoomed perspective of the plot.

GPE, the curve slope presents a slight degree of inclination, which embodies a real electrochemical system with a non-ideal capacitive behavior. This is typical of many systems carrying a polymer electrolyte, where structural characteristics and interactions between ions and polymer chains affect ionic transport and capacitive behavior. Nevertheless, the resistance values (insets of Fig. 1c) at 20, 40 and 80 °C are 64, 28 and 9  $\Omega$ , respectively, which are satisfying values for a quasi-solid system. At –20 °C the resistance contribution is much higher, and a semicircle correlated to charge transfer resistance at medium frequency also appears. Both phenomena are expected from a quasi-solid system [51].

An as wider as possible ESW is fundamental for any proposed novel electrolyte to stably and safely operate within the operational potential of the electrodes. GM-GPE shows an overall ESW of  $\approx 3.1$  V (Fig. 2a), with cathodic and anodic limits of –2.1 and 1 V vs. Ag reference, respectively. Such value is averagely higher than those observed for other methacrylate-based GPEs and other common GPEs [15], making GM-GPE a good candidate for further electrochemical investigations.

Aluminum current collectors are used in EDLCs due to their advantageous combination of low density and weight, high electronic conductivity and low cost. However, in the absence of a protective layer, the anodic dissolution of aluminum can seriously compromise the long-term performance at high operating potentials [52]. In this regard, anodic dissolution tests were carried out on uncoated aluminum discs by holding the potential of the cell at 1.3 V above the open circuit potential of the half-cell while registering the generated current (Fig. 2b). GM-GPE shows an initial increase in current density, reaching approximately 10  $\mu$ A, which could be ascribed to a passivation process at the Al surface or to the initial decomposition of the electrolyte [53].

Nevertheless, no significant current is generated during the test, discarding the hypothesis of anodic dissolution processes at the surface of the Al foil. On the other hand, the current density response of the liquid electrolyte is initially one order of magnitude higher and does not stabilize or decrease during the whole cycling test. It clearly indicates dissolution of the aluminum current collector. The TFSI<sup>–</sup> anions are known to be thermally and electrochemically more stable and less moisture sensitive compared to NaClO<sub>4</sub> and NaPF<sub>6</sub>. However, they also promote the anodic dissolution of aluminum due to the formation of soluble Al(TFSI)<sub>3</sub> [54]. In this regard, encompassing the liquid electrolyte in a crosslinked polymer matrix effectively limits the dissolution process likely due to the restricted solubility of the generated Al(TFSI)<sub>3</sub>. Since the salt is no longer prone to solubilization, it remains on the surface of the electrode, forming a passivation layer, which protects aluminum [55]. The diminished corrosion phenomenon is also confirmed by the FESEM images (Fig. 2c). Normally, anodic dissolution phenomena would be visible through the formation of pitting corrosion signs [54], but in our case no pits or other defects are observed. On the other hand, it was not possible to conduct FESEM analysis on the aluminum current collector of the pure liquid electrolyte cell, since it completely dissolved during measurement. This result highlights the ability of GM-GPE to form a resistant and stable interface, preventing anodic dissolution.

### 3.2. Electrochemical behavior of quasi-solid electric double layer capacitors

GM-GPE was used to fabricate symmetrical laboratory-scale EDLCs, with activated carbon-based electrodes. The EDLCs were initially tested

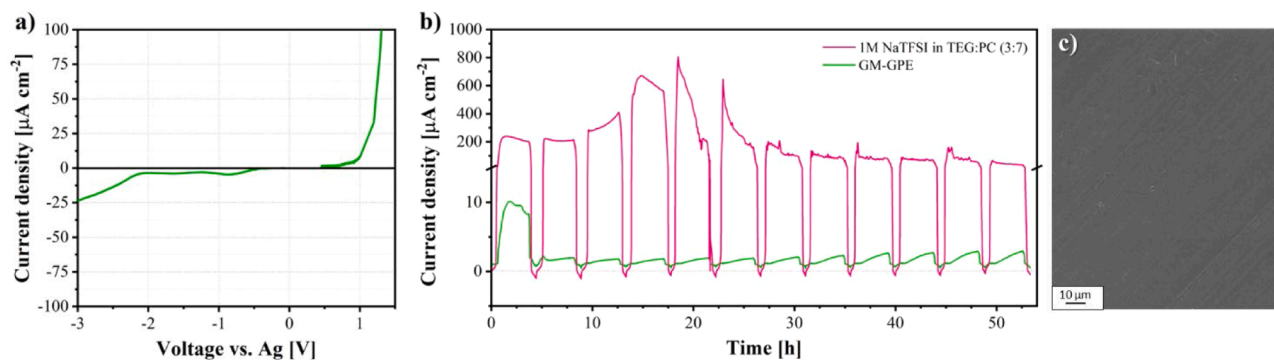


**Fig. 2.** a) ESW of GM-GPE (scan rate: 5 mV s<sup>–1</sup>) with cathodic and anodic limits of –5 and 5 V vs. Ag, respectively. b) Anodic dissolution tests performed for noted electrolytes. c) Post-mortem FESEM image of the Al foil after anodic dissolution tests (1000X magnification).

applying operating voltage in the range of 2 to 3 V (Fig.S1). From these tests, the maximum operating voltage for the investigated systems was set to 2.6 V. Beyond this point, faradaic phenomena can no longer be considered negligible. Ion mobility throughout the GPE was tested by CV at different scan rates (Fig. 3). The rectangular-shaped voltammograms without any visible sign of significant redox reactions reveal the capacitive storage electrostatic mechanism. At low scan rates (5–10  $\text{mV s}^{-1}$ ) the capacitive-like behavior is maintained with comparable values in respect to the liquid system [29] and it is also similar to other devices with different organic solvent-based electrolytes [56]. At higher scan rates, the shape starts to become more elliptic, and the capacitance of the devices slightly drops, which can be ascribed to the resistance of the GPE.

Fig. 4 compares the performances of EDLCs containing the GM-GPE and the corresponding liquid electrolyte. The galvanostatic charge/discharge profiles (Fig. 4a, recorded at a  $0.2 \text{ A g}^{-1}$  current density) reveal that the GM-GPE based cell suffers from a higher ohmic drop, which is related to the higher resistance typical of viscous solid-like systems [57]. At  $0.1 \text{ A g}^{-1}$  the capacitances of the EDLCs containing the two investigated electrolytes were comparable (23 vs.  $28 \text{ F g}^{-1}$  for liquid and GPE; respectively) (Fig.S2). As shown in Fig. 4b, the capacitance retention of the two devices is rather comparable up to  $1 \text{ A g}^{-1}$ . A slightly higher capacitance retention observed with the GM-GPE is likely related to activation processes occurring in the first cycles, leading to an initial increase of the capacitance [58]. Above  $1 \text{ A g}^{-1}$ , however, the higher conductivity of the liquid electrolyte allows a much higher retention than that possible for the GPE-based EDLCs. Fig. 4c compares the energy and power densities of the systems under study in a Ragone plot. As shown, at low current densities ( $0.1 \text{ A g}^{-1}$ ) the energy of the devices is similar and in the order of  $17 \text{ Wh kg}^{-1}$ . The higher resistance of the GPE-based system limits the energy and power densities of the device at higher current densities. At  $1 \text{ A g}^{-1}$  the device containing the liquid electrolyte displays energy and power densities of  $4 \text{ Wh kg}^{-1}$  and  $10,693 \text{ W kg}^{-1}$ , while the values of the GPE-based are  $2.66 \text{ Wh kg}^{-1}$  and  $3924 \text{ W kg}^{-1}$ , respectively. However, taking into account the composition of the electrolyte, these latter values can be considered promising [59]. Furthermore, it is important to remark that the new prepared GM-GPE shows superior thermal stability and safety compared to the liquid counterpart. To further investigate the performance and the stability of the GM-GPE-based EDLCs, a float test at 2.6 V was performed. As shown in Fig. 4d, after 100 h of floating at this voltage, the cell is able to retain above 75 % of its initial capacitance. On the other hand, the EDLC containing the liquid electrolyte shows a continuous decrease in capacitance and overall low retention, with only 40 % of the initial capacitance delivered after 100 h. It clearly evidences the excellent

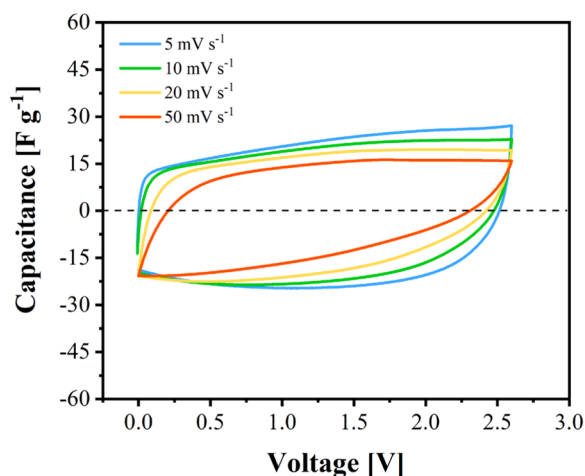


Fig. 3. Cyclic voltammetry of the GM-GPE with a 2-electrode set up with activated carbon, acquired at different scan rates (5, 10, 20 and  $50 \text{ mV s}^{-1}$ ).

stability of GM-GPE and the interfacial stability with the electrode, which minimize degradation phenomena [60]. The initial sudden drop in capacitance is likely correlated to a non-optimal initial contact due to the quasi-solid nature of the system, while following the initial drop the elevated stability indicates a stable interface for the polymer electrolyte. On the contrary, the liquid system shows continuous degradation during float test. Indeed, in the case of the GM-GPE, the capacitance does not only remain stable, but it also tends to increase during the whole measurement indicating the establishment of better interfacial contact.

A long-term galvanostatic stability test was carried out at different current densities for the GM-GPE (Fig. 5). During the initial 1000 cycles at  $0.2 \text{ A g}^{-1}$ , the capacitance of the quasi-solid laboratory-scale EDLC remains above  $21 \text{ F g}^{-1}$ , which is so far in line or even superior in comparison to other reported GPEs prepared for EDLCs [50,61–68]. The assembled EDLC shows a good rate capability when increasing the current rate, with regular limited stepwise decrease up to  $1 \text{ A g}^{-1}$  and only slightly more significant at very high  $2 \text{ A g}^{-1}$ , with 76 and 62 % of the initial capacitance still provided, respectively. After 4000 cycles, when the current density is reduced back to  $0.2 \text{ A g}^{-1}$ , the device still delivers around  $18 \text{ F g}^{-1}$ , which amounts to 85 % of the initial capacitance at the same rate for other 5000 cycles. These results demonstrate the good cycling stability of the GM-GPE.

#### 4. Conclusions

In this paper, BEMA was employed to produce highly crosslinked polymer networks, in combination with PEGMEMA as a reactive diluent. The resulting methacrylate-based membranes were swelled with a glyoxal-based electrolyte, namely  $1 \text{ M NaTFSI}$  in TEG:PC (3:7 in weight), obtaining a glyoxal-methacrylate-based gel polymer electrolyte. In terms of thermal stability, the GM-GPE showed an increased stability in comparison to the liquid system. The ESW resulted to be suitable for energy storage application, but most important, the GM-GPE was able to effectively suppress the occurrence of anodic dissolution of the aluminum current collector. Then, the prepared system was successfully employed as electrolyte in laboratory-scale EDLCs. As typical for (quasi) solid-state systems, the transfer resistance at the interface results in a higher ohmic drop and, thus, in reduced values of specific energy and specific power. On the other hand, ionic conductivity showed satisfactory values and, in terms of capacitance, results were totally comparable to those obtained with the liquid electrolyte based system, even though polymer electrolytes are often linked to a massive decrease in ionic conductivity and capacitance values. Results are promising and pave the way for further detailed studies and optimizations in the field of polymer electrolytes for EDLCs. The remarkable properties of the newly developed GM-GPE make it an interesting candidate also for the realization of (quasi-)solid sodium-ion capacitor and sodium-ion batteries.

#### CRedit authorship contribution statement

**Silvia Porporato:** Writing – original draft, Validation, Investigation, Formal analysis, Conceptualization. **Juan Luis Gómez-Urbano:** Writing – review & editing, Validation, Supervision, Formal analysis, Conceptualization. **Alessandro Piovano:** Writing – review & editing, Writing – original draft, Validation, Supervision, Methodology. **Giuseppe A. Elia:** Writing – original draft, Supervision, Conceptualization. **Claudio Gerbaldi:** Writing – review & editing, Supervision, Resources, Funding acquisition. **Andrea Balducci:** Writing – review & editing, Supervision, Resources, Funding acquisition.

#### Declaration of competing interest

The authors declare the following financial interests/personal relationships which may be considered as potential competing interests:

Claudio Gerbaldi reports financial support was provided by Politecnico di Torino Department of Applied Science and Technology.

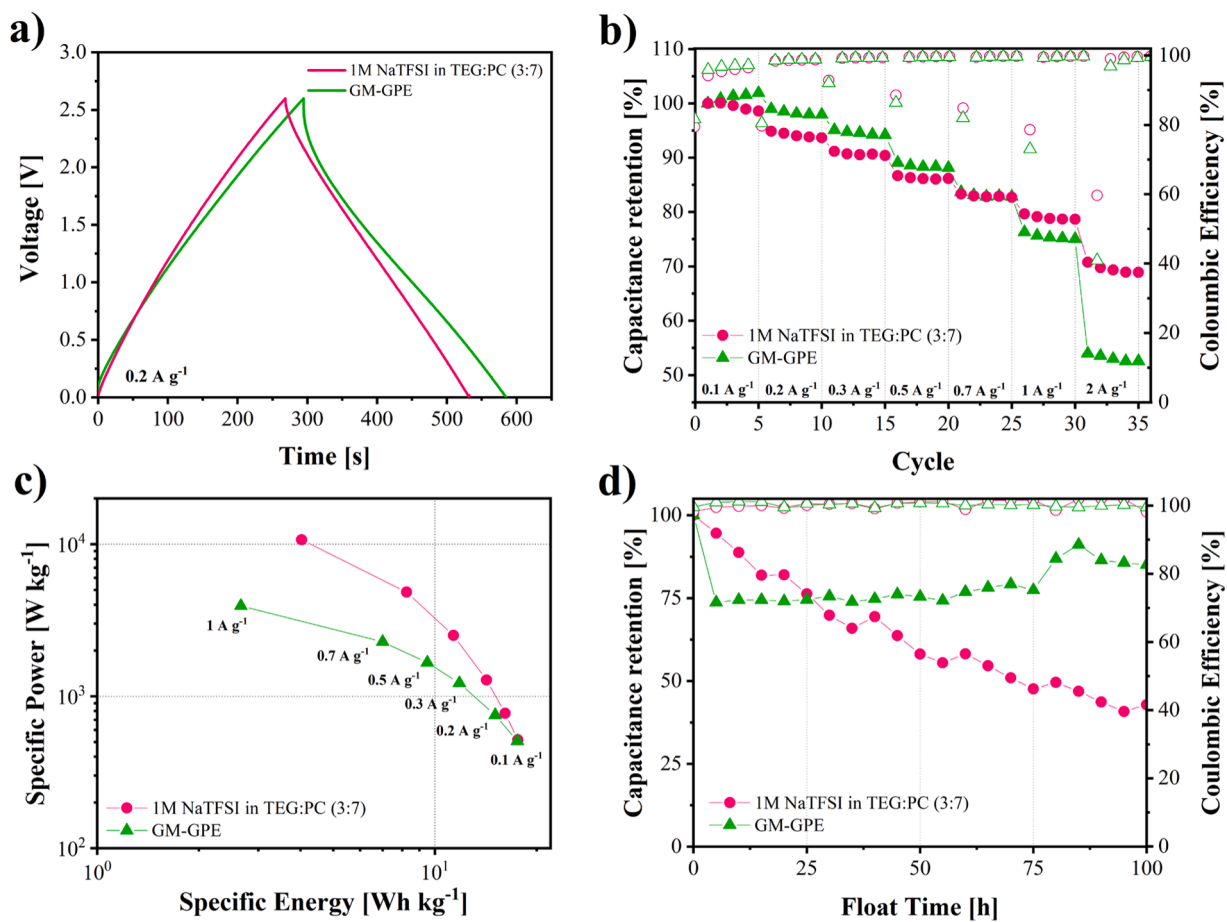


**Fig. 4.** a) Voltage profiles (current density of  $0.2 \text{ A g}^{-1}$ ), b) Variation of capacitance retention and coulombic efficiency of AC-based electrodes in combination with 1 M NaTFSI in TEG:PC (3:7) and the GM-GPE during a rate capability test. c) Ragone plot of the pure liquid electrolyte and the GM-GPE obtained in 2-electrode cell set up with activated carbon electrodes at different current densities ( $0.1, 0.2, 0.3, 0.5, 0.7$  and  $1 \text{ A g}^{-1}$ ). For the calculation of the specific power and specific energy, the active mass in the electrodes has been considered. d) Variation of capacitance retention and coulombic efficiency of AC-based electrodes in combination with 1 M NaTFSI in TEG:PC (3:7) and the GM-GPE during float tests carried out at  $2.6 \text{ V vs. Ag}$  at RT (100 h).

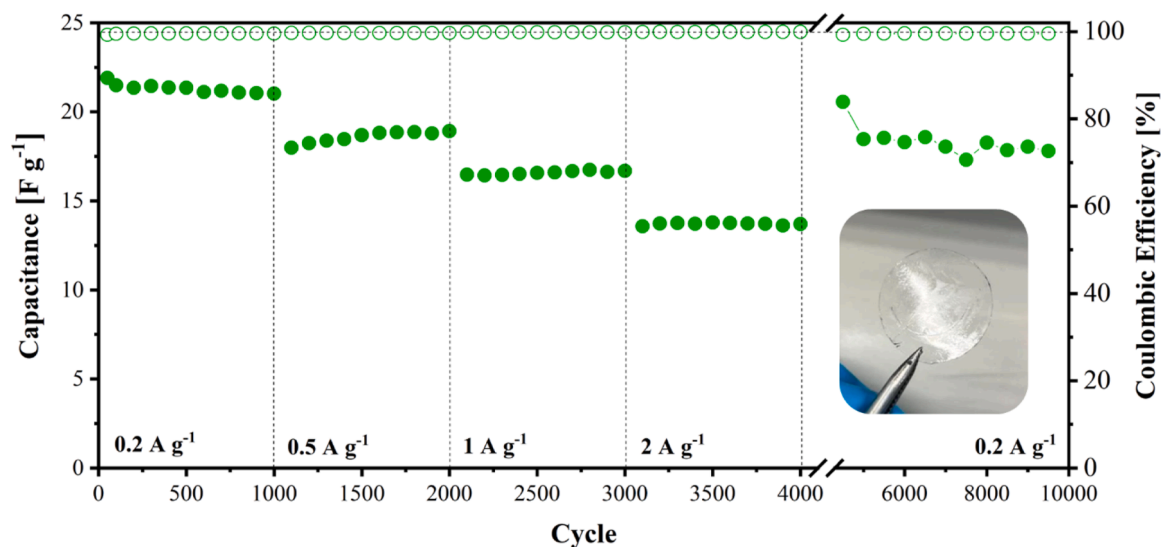


**Fig. 5.** Rate capability test of GM-GPE tested in a symmetrical 2-electrodes cell set up with activated carbon. Inset: digital photograph of the quasi solid-state electrolyte at the end of the cycling test being recovered after cell disassembly.

Claudio Gerbaldi reports a relationship with Polytechnic of Turin Department of Applied Science and Technology that includes: employment. If there are other authors, they declare that they have no known competing financial interests or personal relationships that could have appeared to influence the work reported in this paper.

## Acknowledgements

This study was carried out within the MOST – Sustainable Mobility Center and received funding from the European Union Next-Generation EU (PIANO NAZIONALE DI RIPRESA E RESILIENZA – PNRR – MISSIONE 4 COMPONENTE 2, INVESTIMENTO 1.4 e D.D. 1033 June 17, 2022, CN00000023). A.B and J.L.G.U. want to acknowledge the financial support of the European Union's Horizon Europe transport program under the project SiGNE (grant agreement No 101069738).

A.P. gratefully acknowledges the Italian Ministry for University and Research (MUR) for funding under the D.M. 1062/2021 program. S.P., A.P., G.A.E., and C.G. acknowledge support under the MUR program “Dipartimenti di Eccellenza 2023–2027” (CUPE17G22001490006).

This manuscript reflects only the authors' views and opinions, neither the European Union nor the European Commission can be considered responsible for them.

## Supplementary materials

Supplementary material associated with this article can be found, in the online version, at [doi:10.1016/j.electacta.2025.146096](https://doi.org/10.1016/j.electacta.2025.146096).

## Data availability

Data will be made available on request.

## References

- Z. Yang, J. Zhang, M.C. Kintner-Meyer, X. Lu, D. Choi, J.P. Lemmon, J. Liu, Electrochemical energy storage for green grid, *Chem. Rev.* 111 (2011) 3577–3613.
- M. Hafner, S. Tagliapietra, The Global Energy Transition: a review of the existing literature, in: M. Hafner, S. Tagliapietra (Eds.), *The Geopolitics of the Global Energy Transition*, Springer International Publishing, Cham, 2020, pp. 1–24.
- H. Ibrahim, A. Ilinca, J. Perron, Energy storage systems—Characteristics and comparisons, *Renew. Sust. Energy Rev.* 12 (2008) 1221–1250.
- A.G. Pandolfo, A.F. Hollenkamp, Carbon properties and their role in supercapacitors, *J. Power Sources* 157 (2006) 11–27.
- P. Simon, Y. Gogotsi, Materials for electrochemical capacitors, *Nat. Mater.* 7 (2008) 845–854.
- C. Schütter, T. Husch, M. Korth, A. Balducci, Toward new solvents for EDLCs: from computational screening to electrochemical validation, *J. Phys. Chem. C* 119 (2015) 13413–13424.
- R. Kötz, P. Ruch, D. Cericola, Aging and failure mode of electrochemical double layer capacitors during accelerated constant load tests, *J. Power Sources* 195 (2010) 923–928.
- F. Béguin, V. Presser, A. Balducci, E. Frackowiak, Carbons and electrolytes for advanced supercapacitors, *Adv. Mater.* 26 (2014) 2219–2251.
- J.R. Miller, A. Burke, Electrochemical capacitors: challenges and opportunities for real-world applications, *Electrochem. Soc. Interface* 17 (2008) 53–57.
- P. Azais, L. Duclaux, P. Florian, D. Massiot, M.-A. Lillo-Rodenas, A. Linares-Solano, J.-P. Peres, C. Jehoulet, F. Béguin, Causes of supercapacitors ageing in organic electrolyte, *J. Power Sources* 171 (2007) 1046–1053.
- A. Balducci, Electrolytes for high voltage electrochemical double layer capacitors: a perspective article, *J. Power Sources* 326 (2016) 534–540.
- R. Ramachandran, F. Wang, Electrochemical capacitor performance: influence of aqueous electrolytes. *Supercapacitors - Theoretical and Practical Solutions*, InTech, 2018, pp. 51–68.
- P. Arora, Z. Zhang, Battery Separators, *Chem. Rev.* 104 (2004) 4419–4462.
- J.-C. Wang, W.-J. Zhou, N. Zhang, P.-F. Wang, T.-F. Yi, Review on poly(ethylene oxide)-based solid electrolytes: key issues, potential solutions, and outlook, *Energy Fuels* 38 (2024) 18395–18412.
- J. Zheng, W. Li, X. Liu, J. Zhang, X. Feng, W. Chen, Progress in gel polymer electrolytes for sodium-ion batteries, energy & environmental materials, *Energy Environ. Mater.* 6 (2023) e12422.
- H. Darjazi, M. Falco, F. Colò, L. Balducci, G. Piana, F. Bella, G. Meligrana, F. Nobili, G.A. Elia, C. Gerbaldi, Electrolytes for sodium ion batteries: the current transition from liquid to solid and hybrid systems, *Adv. Mater.* 36 (2024) 2313572.
- C. Gerbaldi, J.R. Nair, G. Meligrana, R. Bongiovanni, S. Bodoardo, N. Penazzi, Highly ionic conducting methacrylic-based gel-polymer electrolytes by UV-curing technique, *J. Appl. Electrochem.* 39 (2009) 2199–2207.
- N.N. Loganathan, V. Perumal, B.R. Pandian, R. Atchudan, T.N.J.I. Edison, M. Ovinis, Recent studies on polymeric materials for supercapacitor development, *J. Energy Storage* 49 (2022) 104149.
- V. Bocharova, A.P. Sokolov, Perspectives for polymer electrolytes: a view from fundamentals of ionic conductivity, *Macromolecules* 53 (2020) 4141–4157.
- Y.G. Cho, C. Hwang, D.S. Cheong, Y.S. Kim, H.K. Song, Gel/solid polymer electrolytes characterized by in situ gelation or polymerization for electrochemical energy systems, *Adv. Mater.* 31 (2019) 1804909.
- C. Gerbaldi, J.R. Nair, G. Meligrana, R. Bongiovanni, S. Bodoardo, N. Penazzi, UV-curable siloxane-acrylate gel-copolymer electrolytes for lithium-based battery applications, *Electrochim. Acta* 55 (2010) 1460–1467.
- C. Gerbaldi, J.R. Nair, S. Ahmad, G. Meligrana, R. Bongiovanni, S. Bodoardo, N. Penazzi, UV-cured polymer electrolytes encompassing hydrophobic room temperature ionic liquid for lithium batteries, *J. Power Sources* 195 (2010) 1706–1713.
- F. Bella, F. Colò, J.R. Nair, C. Gerbaldi, Photopolymer electrolytes for sustainable, upscalable, safe, and ambient-temperature sodium-ion secondary batteries, *ChemSusChem* 8 (2015) 3668–3676.
- J.R. Nair, C. Gerbaldi, G. Meligrana, R. Bongiovanni, S. Bodoardo, N. Penazzi, P. Reale, V. Gentili, UV-cured methacrylic membranes as novel gel-polymer electrolyte for Li-ion batteries, *J. Power Sources* 178 (2008) 751–757.
- S. Emilsson, G. Lindbergh, M. Johansson, Tuneable and efficient manufacturing of Li-ion battery separators using photopolymerization-induced phase separation, *J. Mater. Chem. A* 12 (2024) 30442–30453.
- J.R. Nair, C. Gerbaldi, M. Destro, R. Bongiovanni, N. Penazzi, Methacrylic-based solid polymer electrolyte membranes for lithium-based batteries by a rapid UV-curing process, *React. Funct. Polym.* 71 (2011) 409–416.
- R. He, T. Kyu, Effect of plasticization on ionic conductivity enhancement in relation to glass transition temperature of crosslinked polymer electrolyte membranes, *Macromolecules* 49 (2016) 5637–5648.
- C. Schütter, T. Husch, V. Viswanathan, S. Passerini, A. Balducci, M. Korth, Rational design of new electrolyte materials for electrochemical double layer capacitors, *J. Power Sources* 326 (2016) 541–548.
- L.H. Heß, A. Balducci, Glyoxal-based solvents for electrochemical energy-storage devices, *ChemSusChem* 11 (2018) 1919–1926.
- C. Leibing, D. Leistenschneider, C. Neumann, M. Oschatz, A. Turchanin, A. Balducci, Glyoxylic-acetal-based electrolytes for sodium-ion batteries and sodium-ion capacitors, *ChemSusChem* 16 (2023) e202300161.
- C. Leibing, A. Balducci, Glyoxylic-acetal-based electrolytes in combination with soft and hard carbon electrodes for lithium-ion batteries: an evaluation of room and high temperature performance, *J. Electrochem. Soc.* 168 (2021) 090533.
- L. Köps, C. Leibing, L. Hess, A. Balducci, Mixtures of glyoxylic acetals and organic carbonates as electrolytes for Lithium-ion batteries, *J. Electrochem. Soc.* 168 (2021) 010513.
- S.D. Magar, C. Leibing, J.L. Gómez-Urbano, D. Carriazo, A. Balducci, Brewers' Spent grains-derived carbon as anode for Alkali metal-ion batteries, *Energy Technol.* 10 (2022) 2200379.
- S. Liu, L.C. Meyer, L. Medenbach, A. Balducci, Glyoxal-based electrolytes for potassium-ion batteries, *Energy Storage Mater.* 47 (2022) 534–541.
- M. Klein, M. Binder, M. Kozelj, A. Pierini, T. Gouveia, T. Diemant, A. Schür, S. Brutti, E. Bodo, D. Bresser, J.L. Gómez-Urbano, A. Balducci, Understanding the Role of Imide-Based Salts and Borate-Based Additives for Safe and High-Performance Glyoxal-Based Electrolytes in Ni-Rich NMC811 Cathodes for Li-ion Batteries, *Small* 20 (2024) 2401610.
- A. Bothe, L. Gehrlein, Q. Fu, C. Li, J. Maibach, S. Dsoke, A. Balducci, Glyoxal-based electrolytes in combination with Fe<sub>2</sub>O<sub>3</sub>@C-based electrodes for lithium-ion batteries, *Batter. Supercaps* 5 (2022) e202200152.
- L. Gehrlein, C. Leibing, K. Pfeifer, F. Jeschull, A. Balducci, J. Maibach, Glyoxylic acetals as electrolytes for Si/graphite anodes in lithium-ion batteries, *Electrochim. Acta* 424 (2022) 140642.
- C. Leibing, S. Muench, J.L. Gómez-Urbano, U.S. Schubert, A. Balducci, Glyoxylic-acetal-based gel-polymer electrolytes for lithium-ion batteries, *Batter. Supercaps* 8 (2025) e202400453.
- W. Zaidi, A.I. Boisset, J. Jacquemin, L. Timperman, M. Anouti, Deep eutectic solvents based on N-methylacetamide and a lithium salt as electrolytes at elevated temperature for activated carbon-based supercapacitors, *J. Phys. Chem. C* 118 (2014) 4033–4042.
- T. Evans, J. Olson, V. Bhat, S.-H. Lee, Corrosion of stainless steel battery components by bis(fluorosulfonyl)imide based ionic liquid electrolytes, *J. Power Sources* 269 (2014) 616–620.
- S. Zhou, S. Zhang, S. Wang, W. Zhang, Y. Liu, H. Lin, J. Chen, L. Yan, F. Zhang, H. Li, H. Zheng, Direct evidences for bis(fluorosulfonyl)imide anion hydrolysis in industrial production: pathways based on thermodynamics analysis and theoretical simulation, *J. Power Sources* 577 (2023) 233249.
- Q. Li, G. Liu, Y. Chen, J. Wang, P. Kumar, H. Xie, W. Wahyudi, H. Yu, Z. Wang, Z. Ma, J. Ming, Electrolyte solvent-ion configuration deciphering lithium plating/stripping chemistry for high-performance lithium metal battery, *Adv. Funct. Mater.* (2025) 2420327.
- Z. Tian, Y. Zou, G. Liu, Y. Wang, J. Yin, J. Ming, H.N. Alshareef, Electrolyte solvation structure design for sodium ion batteries, *Adv. Sci.* 9 (2022) 2201207.
- H. Cheng, Q. Sun, L. Li, Y. Zou, Y. Wang, T. Cai, F. Zhao, G. Liu, Z. Ma, W. Wahyudi, Q. Li, J. Ming, Emerging era of electrolyte solvation structure and interfacial model in batteries, *ACS. Energy Lett.* 7 (2022) 490–513.
- J.L. Gómez-Urbano, G. Moreno-Fernández, M. Granados-Moreno, T. Rojo, D. Carriazo, Nanostructured carbon composites from cigarette filter wastes and

- graphene oxide suitable as electrodes for 3.4 V supercapacitors, *Batter. Supercaps* 4 (2021) 1749–1756.
- [46] S. Tillmann, P. Isken, A. Lex-Balducci, Gel polymer electrolyte for lithium-ion batteries comprising cyclic carbonate moieties, *J. Power Sources* 271 (2014) 239–244.
- [47] G.G. Eshetu, S. Grugeon, H. Kim, S. Jeong, L. Wu, G. Gachot, S. Laruelle, M. Armand, S. Passerini, Comprehensive insights into the reactivity of electrolytes based on sodium ions, *ChemSusChem* 9 (2016) 462–471.
- [48] G. Guzmán, D.P. Nava, J. Vazquez-Arenas, J. Cardoso, Design of a zwitterion polymer electrolyte based on poly [poly (ethylene glycol) methacrylate]: the effect of sulfobetaine group on thermal properties and ionic conduction, in: *Macromolecular Symposia*, Wiley Online Library, 2017, p. 1600136.
- [49] J. Vila, P. Ginés, J. Pico, C. Franjo, E. Jiménez, L. Varela, O. Cabeza, Temperature dependence of the electrical conductivity in EMIM-based ionic liquids: evidence of Vogel–Tamman–Fulcher behavior, *Fluid Phase Equilib.* 242 (2006) 141–146.
- [50] T. Stettner, G. Lingua, M. Falco, A. Balducci, C. Gerbaldi, Protic ionic liquids-based crosslinked polymer electrolytes: a new class of solid electrolytes for energy storage devices, *Energy Technol.* 8 (2020) 2000742.
- [51] B.-A. Mei, O. Munteshari, J. Lau, B. Dunn, L. Pilon, Physical interpretations of Nyquist plots for EDLC electrodes and devices, *J. Phys. Chem. C* 122 (2018) 194–206.
- [52] J. Krummacker, L.H. Heß, A. Balducci, Anodic dissolution of Al current collectors in unconventional solvents for high voltage electrochemical double-layer capacitors, *ChemSusChem* 10 (2017) 4178–4189.
- [53] E. Krämer, T. Schedlbauer, B. Hoffmann, L. Terborg, S. Nowak, H.J. Gores, S. Passerini, M. Winter, Mechanism of anodic dissolution of the aluminum current collector in 1 M LiTFSI EC: DEC 3: 7 in rechargeable lithium batteries, *J. Electrochem. Soc.* 160 (2012) A356.
- [54] C. Geng, D. Buchholz, G.T. Kim, D.V. Carvalho, H. Zhang, L.G. Chagas, S. Passerini, Influence of salt concentration on the properties of sodium-based electrolytes, *Small Methods* 3 (2019) 1800208.
- [55] R.-S. Kühnel, M. Lübke, M. Winter, S. Passerini, A. Balducci, Suppression of aluminum current collector corrosion in ionic liquid containing electrolytes, *J. Power Sources* 214 (2012) 178–184.
- [56] C. Zhong, Y. Deng, W. Hu, J. Qiao, L. Zhang, J. Zhang, A review of electrolyte materials and compositions for electrochemical supercapacitors, *Chem. Soc. Rev.* 44 (2015) 7484–7539.
- [57] X. Zhong, J. Tang, L. Cao, W. Kong, Z. Sun, H. Cheng, Z. Lu, H. Pan, B. Xu, Cross-linking of polymer and ionic liquid as high-performance gel electrolyte for flexible solid-state supercapacitors, *Electrochim. Acta* 244 (2017) 112–118.
- [58] A. Lewandowski, A. Świdarska, Solvent-free double-layer capacitors with polymer electrolytes based on 1-ethyl-3-methyl-imidazolium triflate ionic liquid, *Appl. Phys. A* 82 (2006) 579–584.
- [59] J.M. Baptista, J.S. Sagu, U.W. KG, K. Lobato, State-of-the-art materials for high power and high energy supercapacitors: performance metrics and obstacles for the transition from lab to industrial scale—A critical approach, *Chem. Eng. J.* 374 (2019) 1153–1179.
- [60] H. Fei, N. Joseph, E. Vargun, O. Zandrea, M. Omastová, P. Sába, Fabrication and floating test of an asymmetric supercapacitor based on polyaniline and MXene, *Synth. Met.* 300 (2023) 117490.
- [61] S. Poy, S. Bashir, F.S. Omar, N.M. Saidi, N. Farhana, V. Sundararajan, K. Ramesh, S. Ramesh, Poly (1-vinylpyrrolidone-co-vinyl acetate)(PVP-co-VAc) based gel polymer electrolytes for electric double layer capacitors (EDLC), *J. Polymer Res.* 27 (2020) 1–10.
- [62] F. Ramlee, N. Farhana, S. Bashir, N.M. Saidi, F.S. Omar, S. Ramesh, K. Ramesh, S. Ramesh, Electrical property enhancement of poly (vinyl alcohol-co-ethylene)-based gel polymer electrolyte incorporated with triglyme for electric double-layer capacitors (EDLCs), *Ionics* 27 (2021) 361–373.
- [63] S. Shenbagavalli, M. Muthuvinayagam, M. Revathy, Enhancement of electrical and electrochemical properties of sodium bromide incorporated with poly (ethylene oxide)/poly (vinylidene fluoride-hexafluoropropylene) solid blend polymer electrolytes for electrochemical double layer capacitors, *J. Energy Storage* 55 (2022) 105726.
- [64] J.M. Hadi, S.B. Aziz, R.T. Abdulwahid, M.A. Brza, H.B. Tahir, S.M. Hamad, N. Shamsuri, H. Woo, Y. Alias, M.H. Hamsan, O.J.S. Steve, M.F.Z. Kadir, Characterizing sodium-conducting biopolymer blend electrolytes with glycerol plasticizer for EDLC application, *Ionics* 30 (2024) 2409–2423.
- [65] D. Kumar, N. Yadav, K. Mishra, R. Shahid, T. Arif, D. Kanchan, Sodium ion conducting flame-retardant gel polymer electrolyte for sodium batteries and electric double layer capacitors (EDLCs), *J. Energy Storage* 46 (2022) 103899.
- [66] H. Yang, M. Sang, G. Li, D. Zuo, J. Xu, H. Zhang, Stretchable, self-healable, conductive and adhesive gel polymer electrolytes based on a deep eutectic solvent for all-climate flexible electrical double-layer capacitors, *J. Energy Storage* 45 (2022) 103766.
- [67] S.B. Aziz, M.H. Hamsan, R.T. Abdulwahid, N.A. Halim, J. Hassan, A. F. Abdulrahman, S.I. Al-Saeedi, J.M. Hadi, M.F. Kadir, S.M. Hamad, S.R. Saeed, Green Polymer Electrolyte and Activated Charcoal-Based Supercapacitor For Energy Harvesting Application: Electrochemical Characteristics, *Green Process. Synth.* 13 (2024) 20230109.
- [68] N.M. Sadiq, R.T. Abdulwahid, S.B. Aziz, H. Woo, M.F. Kadir, Chitosan as a suitable host for sustainable plasticized nanocomposite sodium ion conducting polymer electrolyte in EDLC applications: structural, ion transport and electrochemical studies, *Int. J. Biol. Macromol.* 265 (2024) 130751.